Indian Journal of Engineering & Materials Sciences
Vol. 31, December 2024, pp. 914-921
DOI: 10.56042/ijems.v31i6.10931

The functionality and features of AI automated detector and counter, Oto-BaCTM for bagworm census in oil palm plantation

Mohd Najib Ahmad[a*], Abdul Rashid Mohamed Shariff[b] & Ramle Moslim[a]

[a]Malaysian Palm Oil Board, 6, PersiaranInstitusi, Bandar BaruBangi, 43600 Kajang, Selangor, Malaysia

[b]Faculty of Engineering, University Putra Malaysia, 43400 Serdang, Selangor, Malaysia

Received:06 May 2024; accepted: 16 September 2024

In Malaysia, the bagworm species *Metisa plana* Walker (Lepidoptera: Psychidae) has been recognized as one of the major insect pests attacking oil palm. Bagworm attacks, if left untreated, have contributed to up to 43% yield loss, and in 2020, the loss of fresh fruit bunches due to these attacks has been chronicled at approximately RM 180 million. Due to this critical situation, it has become compulsory to frequently monitor bagworm infestations in affected areas. Manual census methods, involving the counting of bagworm populations on fronds, have often yielded imprecise data due to human errors, such as overestimating or fabricating data, which have hindered the planning of effective control actions in infested areas. Recognizing the necessity for improved census operations and outcomes, this technology has aimed to create and implement a specialized machine vision system incorporating image processing algorithms tailored to its functions. The device, known as the Automated Bagworm Counter or trademarked as Oto-BaC™, has stood as the world's inaugural prototype in its category. The software has been configured to operate through Graphic Processing Unit (GPU) computation with the TensorFlow/Teano library, utilizing a trained dataset. Oto-BaC™ has employed a standard camera and self-designed deep learning (DL) algorithms, encompassing motion tracking and false color analysis, to identify both living and deceased larvae and pupae of *M. plana*. It has further tallied the respective populations of living and deceased larvae and pupae per frond, classifying them into three primary groups or sizes. This automated device has proven to be straightforward, precise, and user-friendly for bagworm detection and counting on palm leaflets. The technology has relied on advanced deep learning with Faster R-CNN methodology for real-time object detection. Although the instrument has not undergone enumeration testing, it has been crafted to augment bagworm counting efficiency in fieldwork, marking it as the pioneer in its domain. Oto-BaC™'s efficacy and detection precision have been authenticated through a series of field trials conducted at two distinct oil palm plantations afflicted by *M. plana* infestations. Through the integration of infrared sensors and image processing algorithms, this device has been effectively deployed by plantation workers to oversee bagworm populations in their fields, ultimately leading to enhanced yields. This device has exhibited substantial potential for utilization and commercialization, particularly in aiding workers engaged in census-related endeavors.

Keywords: AI automated counter, Bagworm infestations, Census, Deep learning, Precise

1 Introduction

The bagworm, scientifically known as *Thyridopteryxephemeraeformis* (Lepidoptera: Psychidae), is a prominent and severe leaf-eating insect pest in Malaysian oil palm plantations. Previous studies by wood[1] and Basri *et al*.[2] have documented outbreaks of bagworms in these plantations, identifying three main species: *Metisa plana* Walker, *Pteroma pendula* Joannis, and *Mahasena corbetti* Tams. As per the Standard Operating Procedure (SOP) for bagworm control outlined by the Malaysian Palm Oil Board[3] and Najib *et al*.[4], the bagworm has been officially classified as a hazardous pest by the Federal Government Gazette (15 November 2013, P.U. (B) 468) under the Plant Quarantine Act 1976 (Act 167, Section 2). It is considered an offense if a bagworm outbreak is not promptly managed by the plantation owner, leading to penalties under the Plant Quarantine Act 1976. The recommended approach for preventing bagworm outbreaks in oil palm plantations is Integrated Pest Management (IPM). According to the specified bagworm SOP[3], control measures should be implemented when 90% of the bagworm population is in the early larval instars and exceeds the Economic Threshold Level (ETL). For *M. plana* and *P. pendula*, the ETL is set at 10 larvae per frond (LPF).

To effectively manage bagworm infestations in oil palm plantations, it is crucial to perform a census. Presently, this census is carried out manually, relying on visual observation and counting methods. Recognizing the necessity for an improved census method development of Oto-BaCTM is derived from four steps

*Corresponding author (E-mail: mnajib@mpob.gov.my)

a First step - to detect the targeted objects namely bagworms
b Second step – distinguishing between the living and dead bagworms
c Third step – fabrication work of the prototype
d Fourth step – accuracy validation in the field

2 Materials and Methods

The initial phase of this process is centered on bagworm detection, employing a supervised classification algorithm. This algorithm relies on a pre-trained dataset that incorporates specific size and shape criteria to distinguish between different bagworm stages. Experiments were conducted on three distinct groups of *M. plana* Walker, categorized by their developmental stages. The first group consisted of early larval stages, encompassing stages 1 to 3. The second group comprised the late larval stage, spanning stages 4 to 7. The third group encompassed the pupal stage, typically located beneath the oil palm fronds.

In this stage, an algorithm was formulated to identify bagworms and assign them to their respective groups based on their developmental stages. This was accomplished by training the dataset with images for object detection and recognition. A deep learning approach was employed, specifically using Faster R-CNN (Faster Regions with Convolutional Neural Networks), combined with a Region Proposal Network (RPN) as outlined by Ren *et al.*[5]. This method enabled the prediction of object boundaries and object scores at each position. The software operates through GPU computation and is configured with the TensorFlow/Teano library, specifically tailored to the pre-trained dataset.

The second phase involved employing various methods to differentiate between living, dead larvae, and pupae. For distinguishing between living and dead larvae, motion tracking was implemented. The process of motion analysis is outlined as follows:

i The previous frame is processed to serve as the static background image using Background Subtractor MOG2.
ii The current frame undergoes Gaussian Blurring to filter out noise, transforming it into the foreground image.
iii The background image is then masked with the foreground image.
iv The cv2.countNonZero function is applied to the overlapping background and foreground images.
v If there is a nonzero count, it indicates movement in the frame. This signifies the presence of living larvae.

False color analysis was employed to differentiate between living and dead pupae. For this, sixty samples of both dead and living pupae were randomly positioned on a black canvas. Two light sources were chosen for their cost-effectiveness and practicality: 940 nm (infrared) and 630 nm (red). These wavelengths were selected based on the distinctive spectral reflectance characteristics observed in living and dead pupae, particularly between 630 nm and 940 nm. Data on reflectance percentages at specific wavelengths for the pupae was obtained using a spectroradiometer in separate experiments.

Images were captured for both 630 nm and 940 nm in the RGB format. Subsequently, these images were converted into grayscale format. Within the boundary of each pupa, the average values of all the pixels were computed. These average pixel values were then collected for all the samples.

The process for pixel counting is detailed as follows:

a The source image is initially captured in RGB format.
b The position of each pupa is marked to determine the slope value in the red vision (630nm) in contrast to the infrared (940nm) for the pupa at that specific location.
c The image is then displayed in grayscale mode using OpenCV'simshow function (img, imgfile, greyscale_option).
d The view of each pupa is magnified until the pixel value becomes visible.
e Subsequently, all pixels within the pupa image are chosen and their values are averaged.

The third step involves the fabrication of the prototype, Oto-BaC™, which was built up based on the system block design and consists of several key stages. The system consists of interconnected components and modules. All parts, components and modules in the system were designed in 3D CAD software. The overall system design was represented in block diagram shown in Fig. 1 below.

2.1 Mechanical design

- The mechanical design of the prototype was conducted using 3D CAD software to create the enclosure specifications.
- The assembly was carefully planned and set up prior to the fabrication process, which was carried

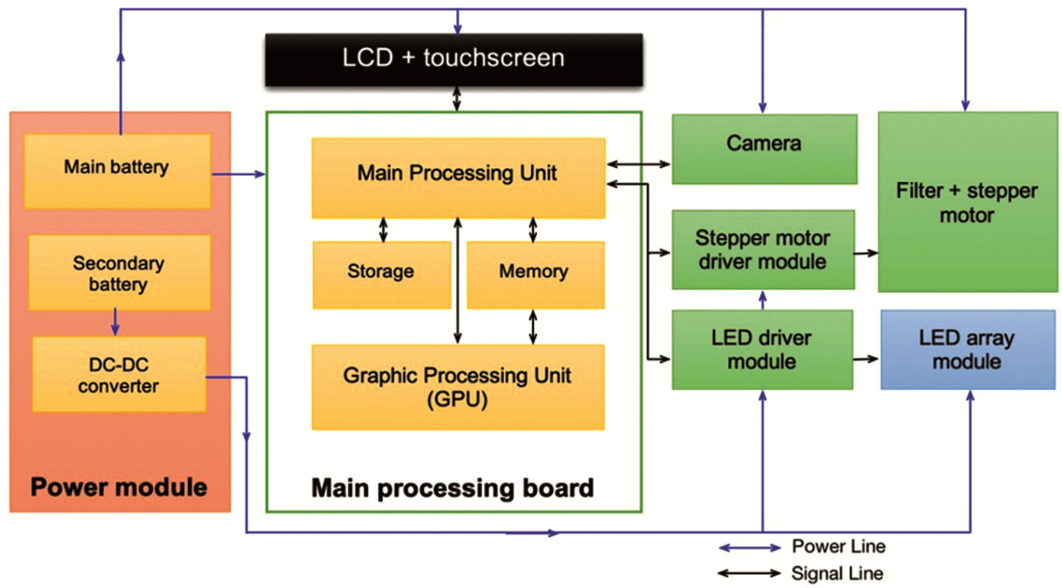

Fig. 1 — Hardware block diagram.

out using a Computer Numerical Control (CNC) machine.

2.2 Device enclosure

- The 3D design of the device enclosure was created using the CAD software.
- Emphasis was placed on user comfort and ease of handling. For instance, the position of the LCD screen was tilted at 15° to offer a clearer view to the user without the need to tilt their head down.

2.3 Computing unit

- The primary processing unit from the Dell Inspiron 7567 model was examined and tested to ensure it met all the necessary criteria.
- The GeForce GTX 1050Ti graphic module having 768 CUDA cores, was considered as moderate in terms of specifications and it was capable to meeting the required processing speed.

2.4 Operating system (OS) and graphical user interface (GUI)

- The fabricated device was equipped with Ubuntu 16.04 64-bit Desktop mode, which is a Linux-based operating system. This OS was chosen to run the Graphical User Interface (GUI), serving as the primary means of interaction between the user and the device.
- A GUI was developed using PyQT5 and Python 3.3. Given that this GUI will instruct another Python file responsible for executing the AI detection algorithm for bagworms, it was essential to ensure that the file locations were consistent for all components.

The fourth step involved the validation of Oto-BaC™'s performance in a real field environment.

2.5 Setup of field trial

The initial field trial took place at Slim River, Perak, on both 17th June 2019 and 8th July 2019, covering an approximate infested area of 1000 hectares. The second field trial occurred on 8th August 2019 in smallholder areas in Tapah, Perak, encompassing a total infested area of 40 hectares. For the field trial, 10 oil palm fronds were selected and cut down. Fronds with an inclination of 45° or those showing signs of attack were chosen for the census, following the guidelines outlined in the bagworm SoP[3]. The field consisted of mature oil palm trees with an average age ranging between 15 to 18 years. The experiment was replicated three times for each treatment in both fields, and a plot size of 8m × 8m was utilized to collect response data. Each frond was divided into three main sections: top, middle, and bottom. Before commencing the test, the field of view (FoV) of the device for each snapshot onto the frond was measured. The number of snapshots required per frond was counted to complete one whole frond census, covering an area of approximately 60cm x 35cm.During the snapshot, the duration of time taken was recorded for both Oto-BaC™ and manual census techniques. It's worth noting that the time duration was influenced by the density of the bagworm population within each FoV slot (for automated counting) or area of interest (AoI) for manual counting.

3 Results and Discussion

The Table 1 displays the performance of the Deep Learning (DL) approach using Faster R-CNN for stage 3 of bagworm detection at various camera distances and conditions.

Based on the data presented in Table 1, it is evident that the Deep Learning (DL) approach utilizing Faster R-CNN outperformed other methods in bagworm detection. The results clearly demonstrate the effectiveness and superiority of the DL technique in this context. The summary is given as follows;

(A) At a distance of 30cm:

- In the Open condition, the algorithm detected 9 out of 10 bagworms (90% detection).
- In the Closed and Half Open conditions, the algorithm detected all 10 bagworms (100% detection).

(B) At a distance of 50cm:

- In the Open condition, the algorithm detected 8 out of 10 bagworms (80% detection).
- In the Closed condition, the algorithm detected 9 out of 10 bagworms (90% detection).
- In the Half Open condition, the algorithm detected 8 out of 10 bagworms (80% detection).

The results indicate a notable distinction in detection accuracy between camera distances of 30 cm and 50 cm, specifically for the closed condition, with statistical significance at $p<0.05$ when compared to the other conditions. In the closed condition, the DL model achieved the highest accuracy, with a recorded rate of 100% at 30 cm and 90% at 50 cm (Figure 2).However, for the open and half open conditions, slightly lower detection rates were observed at both 30 cm (90%) and 50 cm (80%) camera distances. This discrepancy may be attributed to the insufficiency of well-trained data, leading to incorrect detections, which accounted for 10% and 20% of cases at 30 cm and 50 cm, respectively.

According to Fig. 2, distinct image processing techniques were employed for Stage 1&2 and Stage 3, resulting in varying levels of detection accuracy. This was further confirmed by a one-way ANOVA analysis with the Least Significant Difference (LSD) test, indicating statistical significance at $P<0.05$. The color processing technique yielded lower detection accuracy percentages. Specifically, for Stage 1&2

Table 1 — The performance of deep learning in detecting bagworms was evaluated across various camera distances and areas.

Camera distance	Condition	Algorithm detection	Human detection	% detection
30cm	Open	9	10	90 a
30cm	Closed	10	10	100 b
30cm	Half open	9	10	90 a
50cm	Open	8	10	80 a
50cm	Closed	9	10	90 b
50cm	Half open	8	10	80 a

Note: Detection column with different letters denotes significant difference ($P<0.05$) analysed with one-way ANOVA using the LSDtest. Number of bagworms detected depended on randomized leafspots, and the experiment was repeated three times for every condition.

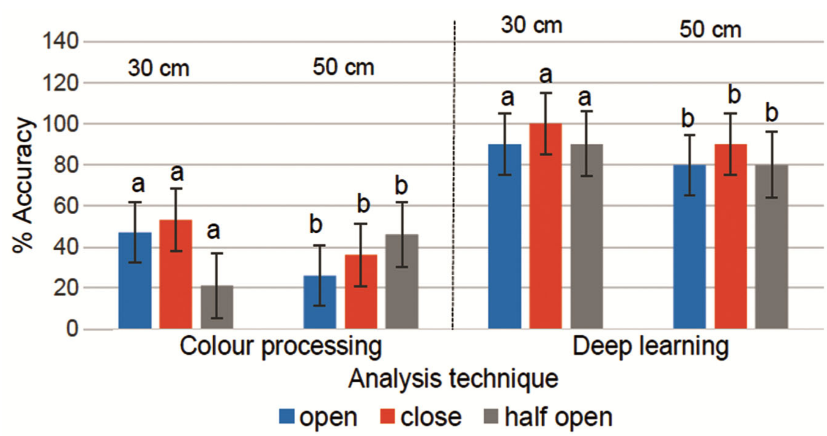

Fig. 2 — This visual representation displays the detection accuracy based on different image analysis techniques corresponding to the Stage 1, 2, and 3 methods at various camera distances. Note: The bars across each group marked with different letters indicate statistically significant differences ($P<0.05$) as determined by the LSD test. This signifies distinct performance levels among the different techniques.

methods, the highest detection accuracy was achieved at 55% for a camera distance of 30cm.

The implementation of the Stage 3 method, which employs Deep Learning (DL), led to a substantial improvement in detection accuracy. Specifically, a remarkable 100% accuracy was achieved at a 30cm camera distance. This suggests that, between both stages, the 30cm camera distance consistently provided superior performance and offered more precise feature details of the bagworms.

The false-color analysis revealed noticeable differences in pixel counts for both dead and live pupae at 630nm and 940nm, aligning with the expected trend based on spectral reflectance properties. Specifically, slopes of 0.37 and 0.26 were recorded for dead and live pupae, respectively. This indicates a positive outcome in distinguishing between living and deceased pupae using the image processing approach. The observed result closely mirrors the trend seen in the spectral reflectance data, albeit with slightly different slope values, as detailed in Table 2. Based on these findings, it is recommended to collect live samples and promptly capture images in the field for optimal results.

Table 2 — The slopes of the reflectance for both living and dead specimens measured using wavelengths of 630nm and 940nm.

Descriptive statistics	Spectral reflectance		False colour imaging	
	Live	Dead	Live	Dead
Mean	0.26	0.38	0.26	0.37
Min	0.26	0.38	0.14	0.30
Max	0.27	0.38	0.29	0.50

Figure 3 demonstrates a significant disparity in slope values between the living and dead pupae. This finding is corroborated by means separation through a Student's t-Test with a significance level set at $p<0.05$.

The primary emphasis in this study lies in validating the effectiveness and precision of Oto-BaC^{TM}. This was established through a series of field trials conducted at two distinct oil palm plantations that were afflicted by *M. plana* bagworms. Based on the data presented in Fig. 2, it was observed that the average percentages of detection and classification accuracy for larval Group 1 and Group 2 in Trial 1 were approximately 48.6% and 41.9%, respectively. In Trial 2, it was approximately 34.9%. These results suggest that there is room for improvement in the detection and classification of these two groups.

During the second field trial, efforts were made to enhance the detection accuracy for larval Group 1 and 2. The results indicated a notable improvement, with an average detection rate of 87.5% for living larvae and 78.7% for dead larvae in Group 1 (refer to Fig. 4). This shows a substantial increase compared to the results of the first trial. In contrast to the initial trial, it was evident that the percentage of detection accuracy saw a significant improvement,

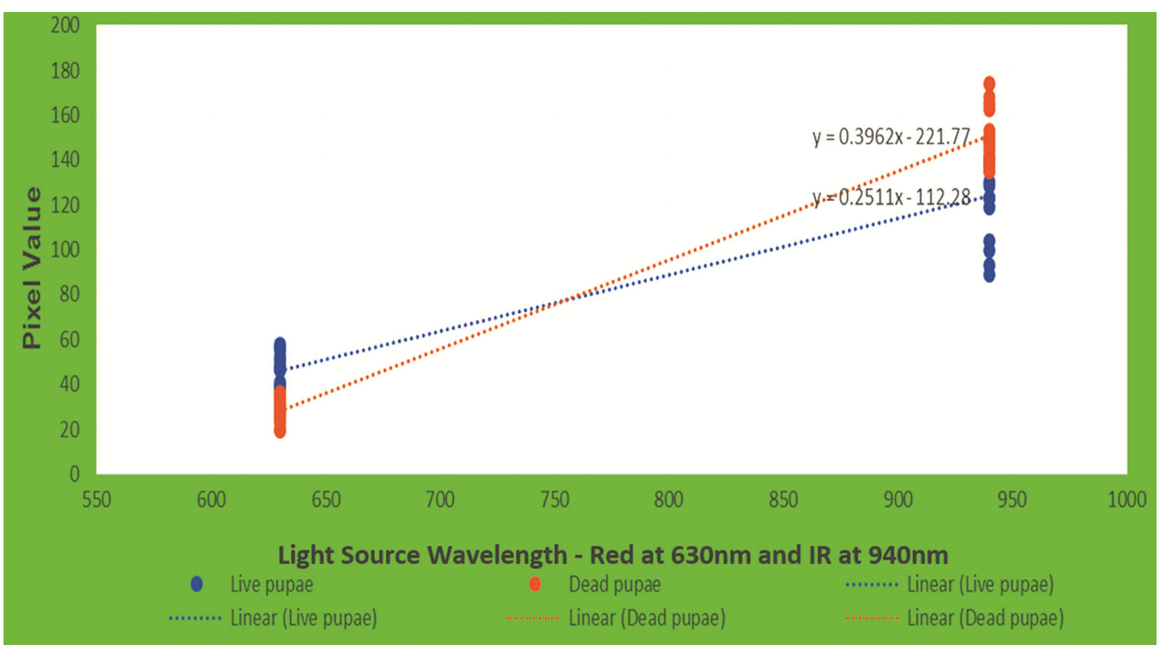

Fig. 3 — The pixel values of the greyscale image were examined using the See3Cam_CU135 camera under two distinct light sources operating at wavelengths of 630nm and 940nm.

with a 40.5% increase for living Group 1 larvae and a 7.0% increase for dead Group 1 larvae. This highlights a promising advancement in detection accuracy achieved through the adjustments made for the second trial.

According to Fig. 4, the outcomes indicate:

- The average percentage of detection accuracy for larval Group 1 was 87.5%, while the classification accuracy was 66.7%.
- For larval Group 2, the average percentage of detection and classification accuracy was 79.2%.

These results demonstrate a substantial improvement in detection and classification accuracy for the improved prototype when compared to the first field trial. In the initial trial, the detection and classification rates were 48.6% and 41.9% for larval Group 1, and 34.9% for larval Group 2 (as shown in Fig. 4). Furthermore, in Fig. 5, it is observed that the average detection accuracy increased to 77.8% for living pupae and 75.5% for dead pupae. This indicates a notable enhancement in detection accuracy for both living and dead pupae compared to previous results.

According to Fig. 5, the average percentage of detection accuracy for both living and dead G2 larvae was recorded at 79.2%. This indicates a notable positive outcome, with a substantial 40.1% increase in detection accuracy for living G2 larvae and a 29.2% increase for dead G2 larvae when compared to the results of the first trial.

In summary, significant detection improvement, with a statistical significance level of $p<0.05$ as confirmed by the LSD test (Table 3), was observed

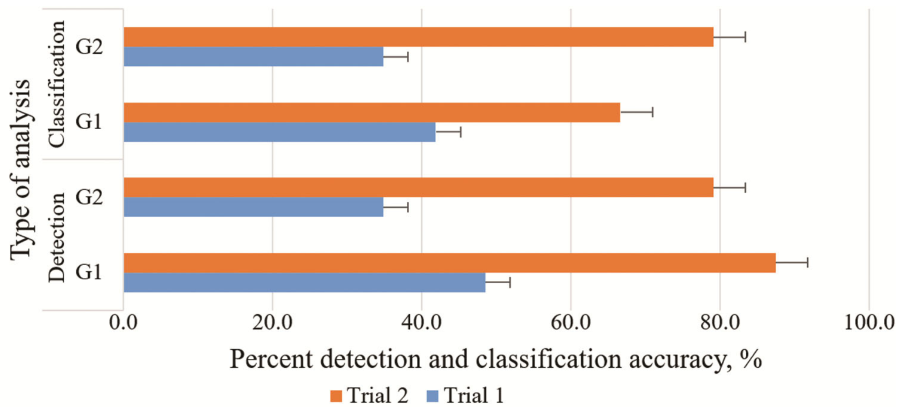

Fig. 4 — Summary of analysis on detection and classification of the living and dead larval Groups 1 and 2 in Trials 1 and 2.

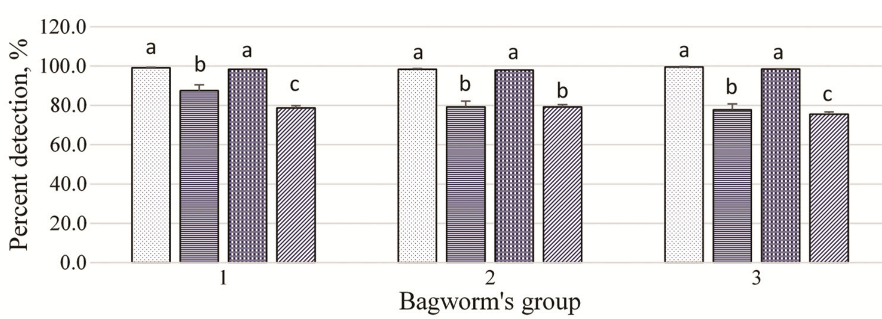

Fig. 5 — The improved prototype's overall performance in detecting living and dead bagworms through automatic census, as compared to manual census in the second trial, is depicted in the provided visual representation. Note: Bars within a group marked with different letters signify statistically significant differences (P<0.05) as determined by the LSD test. This indicates distinct performance levels among the different methods.

Table 3 — A summary of bagworm detection accuracy using Oto-BaC^{TM}for G1-G3 groups in two trials

Group	% Detection in Trial 1		% Detection in Trial 2		% Improvement		Census duration, min/frond	
	Live	Dead	Live	Dead	Live	Dead	Automatic	Manual
1(larvae)	47.0a	71.7a	87.5b	78.7b	40.5	7.0	14.0	17.2
2(larvae)	39.1a	50.0a	79.2b	79.2b	40.1	29.2	13.9	17.0
3(pupae)	30.1a	20.9a	77.8b	75.5b	47.7	54.6	0.5	0.8

Note: Column across a trial group with different letters denote significant difference (P<0.05) after least significant difference (LSD) test.

between the first and second trial. These improvements were observed when the two trials were conducted at two different locations.

Table 3 underscores a significant distinction in the percentage of detection between the first and second trials for both living and dead bagworms. Notably, Group 3 exhibits a substantial improvement in percentage, with 47.7% for living pupae and 54.6% for dead pupae. This is attributed to the size effect of pupae in comparison to G1 and G2 larvae. The distinct size and location of the pupae on the palm leaflet's bottom part provided an advantage for Group 3. These two factors worked synergistically to prevent overlapping detection by the algorithm, resulting in a high percentage of detection for G3 pupae.

Furthermore, the census duration for a complete frond was recorded for G1 larvae, G2 larvae, and G3 pupae using the prototype (Oto-BaC™) and manual census. It was observed that the census duration for G1 and G2 larvae was longer compared to G3, primarily due to the different detection techniques applied. This indicates that the detection process was more efficient for G3 pupae.

The results from the first field trial indicate that distinguishing between living and dead bagworms presented a significant challenge. The detection accuracy for G1 larvae ranged from approximately 47% to 72%, while for G2 larvae, it ranged from around 39% to 50%. This aspect proved to be the most demanding, primarily because the prototype's performance was assessed at the actual field site of oil palm plantations, where there was an ongoing bagworm outbreak. Additionally, accounting for the varying lighting conditions from the surroundings and sunlight, the prototype was equipped with an imaging chamber or operated within a closed system setup to mitigate these effects[6]. This condition gave a better recognition on bagworm features or details. The detection accuracy was inconsistent throughout all tests. Some tests showed higher score while some obtained lower score. After analysis is performed, it was found out that the detection and classification is not consistent throughout all 100 images/frames. In some condition, on current frame, the algorithm does not detect bagworm at one exact particular coordinate, but detect it on the previous and the next frames. When tests were conducted, the counting algorithm was based on the average counts. The accuracy become lower when the algorithm detects less bagworm on majority of the frames. The detection results for G1 andG2 using first version algorithm was developed during the software development phase. An improvement has been made to the counting algorithm as following[7]:

New Counting Algorithm:

i Running detection algorithm on current frame to get and save all bagworm coordinates.
ii Running detection algorithm on the next frame to get and save all bagworm coordinates.
iii Using non-maximum suppression technique to filter any redundant bagworm coordinates from saved coordinates. If coordinates redundant then remove duplicates redundant.
iv Repeat step above until complete all frames.
v Count the final saved bagworm coordinates to know the bagworms count.

The new counting algorithm was further used in second trial to validate effectiveness of the trained dataset with new images. The results from the second field trial demonstrate significant improvements in detection percentages:

- For larval Group 1 (G1), the detection rate increased to an impressive 87.5%.
- For larval Group 2 (G2), the detection rate increased to 79.2%.
- Notably, even for the pupal stage (G3), there was a substantial increase in detection accuracy, reaching up to 77%.

These advancements were achieved through a combination of measures, including the incorporation of additional image datasets for training and the implementation of an updated algorithm specifically tailored for detecting living larvae. This approach yielded substantial improvements in detection performance across all stages.

Shivang *et al.*[8] suggested that up-scaling the image prior to detection can potentially mitigate issues associated with low detection rates. This approach can help enhance the visibility of smaller objects or features within the image. However, it's worth noting that while up-scaling may be effective for improving detection, it does come with its own set of challenges. An up-scaling may lead to significantly larger images that may become impractical for processing, especially when it comes to training deep learning models on GPUs. The increased size and complexity of the data may strain computational resources and slow down the training process. Therefore, finding a balance between up-scaling for improved detection and managing computational resources is a critical consideration in image processing and object detection tasks.

Specificity of the model through train model from Faster R-CNN Resnet 101 that can detect smaller objects can increase detection accuracy. To further study the reason behind low accuracy, a smaller lens field of view (FOV) was used to capture images with effect of two times (2x) zoom. When this lens was used, the area captured by camera will be half the original images captured using the existing lens. However, the image size is still same as the resolution setting was unchanged. With smaller captured area, the bagworm's detail will be greater. This can provide distinctive feature to the algorithm to differentiate a bagworm in the frame from others. The new lens used has aperture value F5.6 and focal length 2.7mm from Edmund Optics. Zhao *et al.*[9] highlight a crucial point: the size and quality of the training data play a pivotal role in the performance of a detection model. A larger and more diverse training dataset enables the model to learn a wider range of features and patterns, ultimately leading to improved accuracy and generalization ability. This principle is fundamental in machine learning and deep learning, where the quality and quantity of training data have a direct impact on the model's effectiveness.

4 Conclusion

The software and hardware for bagworm automatic detection and counting had been developed, fabricated and tested on field. The accuracy of detection for the prototype device has been improved since the inception until it reached acceptable accuracy level. However, it was observed that, several train data when tested using the same images, some bagworms not detected by the algorithm even though the bagworms have been labelled during training. These occurred for both initial lens and new lens with smaller FOV. Changing train model from Faster RCNN Resnet 101 in some models can detect smaller objects could solve this issue as well as improve the accuracy. However, changing a train model will require repetition of processes from the beginning with image label and rerun training session as the frozen training data may not work and interchangeable.

Acknowledgments

The authors would like to thank the Director-General of the Malaysian Palm Oil Board (MPOB) for permission to publish this article, the financial support and patenting of all data. Much gratitude also goes to University Putra Malaysia (UPM), Selangor, Malaysia for technical and supervisory support throughout the study.

References

1 Wood B J, Pests of Oil Palms in Malaysia and Their Control (Wiley Online Library, Malaysia),1968, 1st Edition, p. 204.
2 Basri M W, Abdul H H & Zulkifli M, *PORIM occasional paper*, 23 (1988)37.
3 Malaysian Palm Oil Board, Standard Operating Procedures (SoP) Guidelines for Bagworm Control (Malaysian Palm Oil Board, Malaysia)ISBN 978-967-961-218-9, 2016, p. 20.
4 Najib M A, Ramle M & Rashid AMS, An Automated Artificial Intelligence (A.I.) Counter for Bagworm (Lepidoptera: Psychidae) Census (Malaysian Palm Oil Board Information Series, Malaysia) ISSN 1511-7871, 2020, p. 9.
5 Ren S, He K, Girshick R & Sun J, *Adv Neural Inform Sys*, 25 (2015) 91.
6 Najib MA, Rashid AMS, Ishak A&Izhal AH, *Adv Agri Food Res J,* 2 (2021b) 17.
7 Najib MA, Rashid AMS, Ishak A & Izhal AH, *Agriculture,*11 (*2021a)* 1265.
8 Shivang A, Jean ODT & Frédéric J, Recent Advances in Object Detection in the Age of Deep Convolutional Neural Networks (HAL Open Science, France)HAL Id: hal-01869779, 2019, p. 105.
9 Zhou S, Xu Z, Liu L, Guo M & Yun J, *Mathemat Prob Eng*, 2018 (2018) 9.